Asian Journal of Chemistry; Vol. 34, No. 7 (2022), 1703-1710

ASIAN JOURNAL OF CHEMISTRY

https://doi.org/10.14233/ajchem.2022.23660

Green Synthesis of Copper Nanoparticles and Evaluation of its Antioxidant and Antibacterial Efficacy

MD. MOULANA KAREEM[1,2] and G. VIJAYA LAKSHMI[2,*]

[1]Department of Chemistry, Government Degree College, Manuguru-507117, India
[2]Department of Chemistry, Osmania University College for Women, Hyderabad-500095, India

*Corresponding author: E-mail: gvjlakshmi@gmail.com

Received: 14 November 2021; *Accepted*: 21 February 2022; *Published online*: 15 June 2022; AJC-20844

The current study presents a simple and green method for the optimal synthesis of copper nanoparticles (CuNPs) using $Cu(CH_3COO)_2$ and aqueous extract of *Terminalic chebula* fruit as a reducing and capping agent. UV-vis spectroscopy absorbance at 580 nm was used to characterize the resultant CuNPs. Further FT-IR analysis revealed that the existence of phytochemicals, which reduce Cu^{2+} ions to Cu and stabilize the resultant CuNPs. Transmission electron microscopy (TEM), scanning electron microscopy (SEM) and X-ray diffraction (XRD) were employed to investigate the shape and crystalline phase of CuNPs. The CuNPs were spherical in shape and averaged 23.68 nm in size. The copper nanoparticles inhibited Gram-negative *E. coli* more efficiently than Gram-positive *S. aureus* with the inhibition zones of 14.5 and 9.2 mm, respectively. Furthermore, these CuNPs exhibited dose-dependent free radical scavenging activity, with an EC_{50} for DPPH of 44.65 µg/mL.

Keywords: Antibacterial, Eco-friendly, *Terminalic chebula,* Phytochemicals, Scavenging activity.

INTRODUCTION

The biological synthesis of nanoparticles has grabbed the attention of researchers from different fields like material science, life science, medicinal science, biotechnology, physics, chemistry, pharmaceutics and various industries and has become a certain and promising area of scientific and technological development for the coming days [1,2]. Nanotechnology represents the design, production and application of materials at atomic, molecular and macromolecular scales to produce new nano-sized materials [3,4].

Among the various metal nanoparticles, copper nanoparticles are widely used in medical devices, electronic devices, heat transfer systems, biosensors, pharmaceutical industries for drug-eluting and as reagents in various reactions, lubricants, food packaging industries, antibiotics, antimicrobial agents, as catalysts in many reactions and a variety of other applications [5-7]. Several studies have found that the phytochemicals mediated CuNPs are more mobile in the environment, interacting with and passing through bacterial membranes [8].

The copper nanoparticles can be synthesized by different methods such as physical, chemical and biological (green) method. Green synthesis approaches for nanoparticle manufacturing rely on living organisms and biological precursors such as actinomycetes, fungus, bacteria, yeast, viruses and plant components [9]. However, the use of green resources such as plant components, enzymes, microorganisms, *etc*. not only avoids the use of toxic chemicals but is also more efficient, simpler and less expensive [10]. This greener approach of producing metal nanoparticles is advantageous due to its readily availability, environmentally friendly and results in arduous purification steps [11].

Biological entities offer a non-toxic and eco-friendly method for converting metal ions into metal nanoparticles with a diverse variety of sizes, physico-chemical properties, morphologies and compositions [12]. Enzymes, proteins, saponins, tannins, flavonoids, alkaloids, steroids and terpenoids are all found in plant components and have therapeutic effects. These metabolites include reactive groups with significant reducing capacities and can thus be utilized to produce metal nanoparticles [13]. Several articles described studies on the synthesis of copper nanoparticles from various plant resources including ginger [14], oleander leaves [15], arevalanata leaves extract [16], eucalyptus plant leaves extract [17], *Capparis zeylanica*

leaves extract [18], *Citrus medica* Linn. [19], Euphorbia equal leaves [20] and cloves extract [21].

Terminalia chebula Retz. belongs to *Combretaceae* family and its dried fruit is used in Ayurveda for treatment of asthma, piles, sore throat, vomiting and gout [22]. Its extract contains phytochemicals such as polyphenols (chebulic acid), which is a water-soluble tannin that aids *in situ* nanoparticle synthesis and oxidized polyphenols may act as capping agents [23]. Nevertheless, copper nanoparticles synthesis using *T. chebula* fruit aqueous extract and $Cu(CH_3COO)_2$ solution has not been reported earlier. The objective of this study was to synthesize stable CuNPs from *T. chebula* fruit aqueous extract and then evaluate their antibacterial and antioxidant properties against human pathogen bacteria and DPPH.

EXPERIMENTAL

Copper acetate, sodium hydroxide, DPPH (2,2-diphenyl-1-picrylhydrazyl), methanol, ascorbic acid, of analytical grade were purchased from Sigma-Aldrich India, while Mueller-Hinton Agar and sterilized discs were procured from Hi-media, India. *Terminalia chebula* fruits were acquired from the local market.

Preparation of aqueous extract of *T. chebula* fruit: *T. chebula* fruit was thoroughly washed, chopped and dried before being powdered and placed in an airtight bag for experiments. Approximately 1 g of powder was transferred in a clean 250 mL conical flask containing 100 mL of double distilled water and swirled with a magnetic stirrer for 30 min at 60 ºC. The extract was then cooled to room temperature and filtered through Whatmann no.1 filter paper. The filtrate was centrifuged at 4000 rpm for 15 min. Finally, the recovered fruit extract filtrate was kept at 4 ºC for further use [23].

Optimal conditions for the biosynthesis of copper nanoparticles: In order to identify optimal conditions, the synthesis of CuNPs using *Terminalia chebula* fruit aqueous extract was investigated using various parameters such as pH (2,4,6 and 8), precursor concentration (1, 2, 3 and 4 mM), temperature (20, 40, 60, 80 and 100 ºC) and time (20, 30, 40 and 50 min). The pH of the reaction medium was adjusted with 0.1 N NaOH and 0.1 N HCl. The influence of these parameters was monitored using a UV-visible spectrophotometer with a wavelength range of 400-800 nm.

Biosynthesis of copper nanoparticles (CuNPs): As per optimization study, 10 mL of *T. chebula* aqueous extract was mixed with 90 mL of 3 mM $Cu(CH_3COO)_2$ solution in a clean 250 mL conical flask. The pH of the reaction mixture was adjusted to 6 using 0.1 N HCl solution and the mixture was heated at 60 ºC for 50 min on a magnetic stirrer. After allowing the reaction mixture to cool to room temperature, it was centrifuged for 20 min at 4000 rpms, with the supernatant removed to collect the residue. This residue was dispersed twice with double distilled water before drying in an oven at 80 ºC for 1 h [24].

Characterization: Synthesized CuNPs were characterized by using UV/Vis spectroscopy (LAB INDIA UV-3000+)), Fourier transform infrared spectroscopy (FTIR, Shimadzu), zeta potential (Zetasizer Nano ZS90), X-ray diffraction (X-RD, Bruker D8 Advance with Cu$K\alpha$), scanning electron microscopy (Carl Zeiss model Ultra 55 microscope), energy dispersive of X-ray (EDX) nalysis (Oxford Instruments X-MaxN SDD (50 mm2) system interfaced at 5 kV and INCA analysis software) and TEM (JEOL JEM-2100F instrument equipped with a slow-scan CCD camera and an accelerating voltage of the electron beam of 200 kV).

Determination of antioxidant activity using DPPH (2,2-diphenyl-1-picrylhydrazyl) assay: The DPPH assay was used to assess the free radical scavenging activity of biosynthesized TC-CuNPs, based on the slightly modified methodology [25]. DPPH (4 mg) was dissolved in 100 mL methanol to make the 4% DPPH solution. As DPPH is particularly photosensitive, the DPPH solution produced was immediately enveloped in aluminum foil and stored in the dark. The dilution series of reaction mixture was prepared using different concentrations of biosynthesized CuNPs (10-50 µg/mL) and incubated with DPPH (3 mL; 4 mM) solutions in methanol for 30 min, the solution was allowed to stand at room temperature. A UV-visible spectrometer was used to assess the absorbance of the control (without CuNPs) and test samples at 517 nm. Ascorbic acid is used as a standard antioxidant [24].

The % inhibition of DPPH calculated by the following formula:

$$\text{Inhibition of DPPH (\%)} = \frac{C - T}{C} \times 100$$

where C is the absorbance of control and T is the absorbance of the test sample.

Antibacterial activity: Antibacterial activities of CuNPs were evaluated using agar disc diffusion method on Mueller Hinton agar (MHA). *S. aureus* (ATCC 25923) and *E. coli* (ATCC 25922) were used as references single colonies from overnight grown culture on agar plates were used to prepare the bacterial suspension with the turbidity of 0.5 McFarland (equal to 1.5×10^8 CFU/mL). Turbidity of the bacterial suspension were measured at 600 nm. Individual Petri dishes with 20 mL of molten nutrient agar were filled and allowed to cool, then swabbed with a fresh overnight culture from each strain on sterile and cooled MHA [26]. Following that, 6 mm diameter sterile discs were impregnated with different amounts of CuNPs (40, 60, 80 and 100 L) using sterile micropipette. The discs filled with the corresponding bacteria alone were used as a control in each Petri dish [27]. The impregnated discs were placed on petri plates and incubated for 24 h at 37 ºC. Following the incubation period, the antimicrobial activity was assessed by measuring the inhibition zones produced around the discs in millimeters (mm).

Minimum inhibitory concentration (MIC): The MIC assay was determined by microdilution method. The well plates were prepared by dispensing 100 µL of nutrient broth into each well. Stock solution (100 µL) of tested nanoparticles (50 mg/mL) and added into the first well of the plate. Then, two-fold serial dilutions were performed by using a micropipette. The obtained concentration range was from 50 mg/mL and then added 50 µL of inoculum to each well except negative

control. The positive control of antibiotic (ampicillin), negative control (nutrient broth), broth alone and the inoculum alone were also examined. The test plates were incubated at 37 ºC for 24 h. The lowest sample concentration showing clear well and inhibited complete growth were taken as MIC value [28].

RESULTS AND DISCUSSION

UV-visible studies: Typically, the UV-visible absorbance spectrum is utilized to confirm the formation of nanoparticles. Fig. 1 shows that the CuNPs had a wide peak about 580 nm, suggesting the presence of stable and well distributed CuNPs. The surface plasma resonance of CuNPs free electrons causes this absorption band. These changes in SPR can be related to the spherical shape of copper nanoparticles, as the surface plasmon resonance and blue shift are influenced by size distribution, results in a single SPR band in the absorption spectra of spherical metal nanoparticles [29]. A single SPR peak was found in the current investigation, assuming that the produced CuNPs were spherical in form.

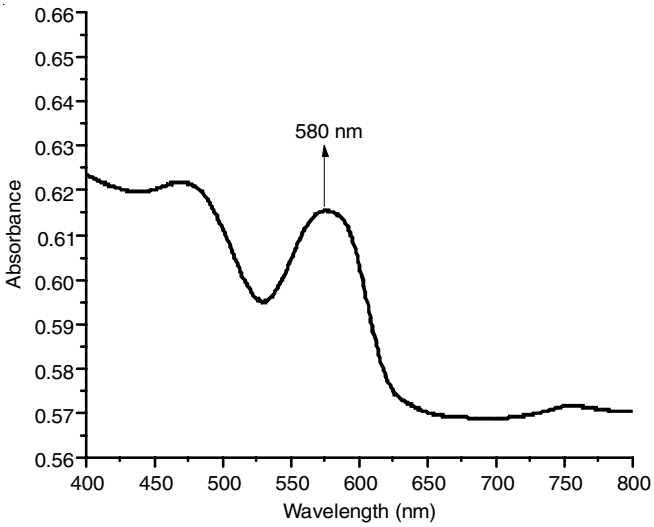

Fig. 1. UV-visible spectra of biosynthesized CuNPs

The optimal conditions for the biosynthesis of CuNPs using *T. chebula* fruit aqueous extract were found using a UV-visible spectrophotometer with a wavelength range of 400-800 nm, as measured by peak position and intensity. SPR peaks at longer wavelength regions (red shift) are produced by bigger nanoparticles, whereas SPR peaks at shorter wavelengths are produced by smaller nanoparticles (blue shift) [30].

Optimal precursor concentration: The formation of copper nanoparticles was studied by the variation of copper acetate concentration from 0.5 to 4 mM. The UV-visible spectrum was recorded for the change in SPR peaks position with variation in the precursor salt concentration as shown in the Fig. 2a. An increase in concentration from 0.5 mM to 3 mM induced a blue shift in wavelength from 590 to 580 nm, which was associated with an increase in peak intensity, but an increase in concentration to 4 mM caused a red shift from 580 to 615 nm, which was coupled with a decrease in peak intensity. It may be believed that when the concentration of copper acetate increases above 3 mM, the SPR absorbance decreases, possibly due to a low number of reducing agent molecules. The number of Cu^{2+} ions that must be reduced to Cu nuclei is less when the concentration of copper acetate is low (0.05 mM) [31]. As a consequence, the optimal concentration of copper acetate was determined to be 3 mM.

Optimal pH: The green synthesis of copper nanoparticles using aqueous extract of *T. chebula* fruit was examined across a wide pH range (2-8). The SPR of CuNPs is significantly affected by pH changes. Increasing the pH from 2 to 6 leads a blue shift in wavelength from 588 to 580 nm, resulting in an increase in peak intensity (Fig. 2b). However, increasing the pH from 6 to 8 resulted in a red shift from 580 to 620 nm, as well as a decline in peak intensity. The peak's absorption intensity in the UV-visible spectra was maximum at pH 6. In general, acidic pH zones can induce biomolecules in the extract to become inactive, resulting in formation of smaller nanoparticle [32]. As a result, pH 6 was found to be optimal for the biosynthesis of CuNPs.

Optimal temperature: According to Fig. 2c, the optimal temperature was 60 ºC because it produced the sharpest and most intense peak. This may be explained by the fact that at higher temperatures, the rate of nucleation takes precedence over the rate of growth [33].

Optimal reaction time: Fig. 2d depicts the UV-visible spectra of CuNPs as a function of time. The time period of 50 min was considered optimal because it yielded the sharpest and most intense peak.

FTIR analysis: The FTIR spectrum of *T. chebula* fruit aqueous extract (Fig. 3) revealed bands at 3367, 1790, 1643, 1399, 1191, 1020, 933 and 874 cm^{-1} arose due to stretching's of –O-H, –N-H, –C=O and C-O-C bonds, which in turn indicate the presence of secondary metabolites such as phenolics, flavonoids and carbohydrates in the extract. The FTIR spectrum of CuNPs revealed a decline in peak intensity as well as a shift change in peak location of –OH, –NH and –C=O bands indicating the reduction and stabilization of CuNPs by these groups [34].

Zeta potential: The charge determined by zeta analysis was -28.1 mV as shown in Fig. 4. Particles having zeta potentials larger than ± 25 mV are thought to be more stable. Particles with negative charges have a high repulsion force between them. This demonstrates the qualities of stability and quality [35].

XRD analysis: Fig. 5 depicts the X-ray diffraction pattern of biosynthesized CuNPs. CuNPs exhibit prominent peaks at position 2θ values of 43.083º, 50.218º and 73.917º, which are readily indexed the reflection planes (111), (200) and (220) from the XRD patterns, respectively. The obtained values of three peaks, as given in Table-1, are quite near to the standard JCPDS card No. 04-0836 [36]. The mean crystalline size (D) of CuNPs was calculated using Debye Scherrer's formula. The average crystallographic dimension (D) of CuNPs was found to be 23.28 nm, which are similar to the TEM findings.

Scanning electron microscopy (SEM) analysis: The morphological characterization of CuNPs was carried out using SEM-EDS and TEM analyses. The SEM analysis revealed the

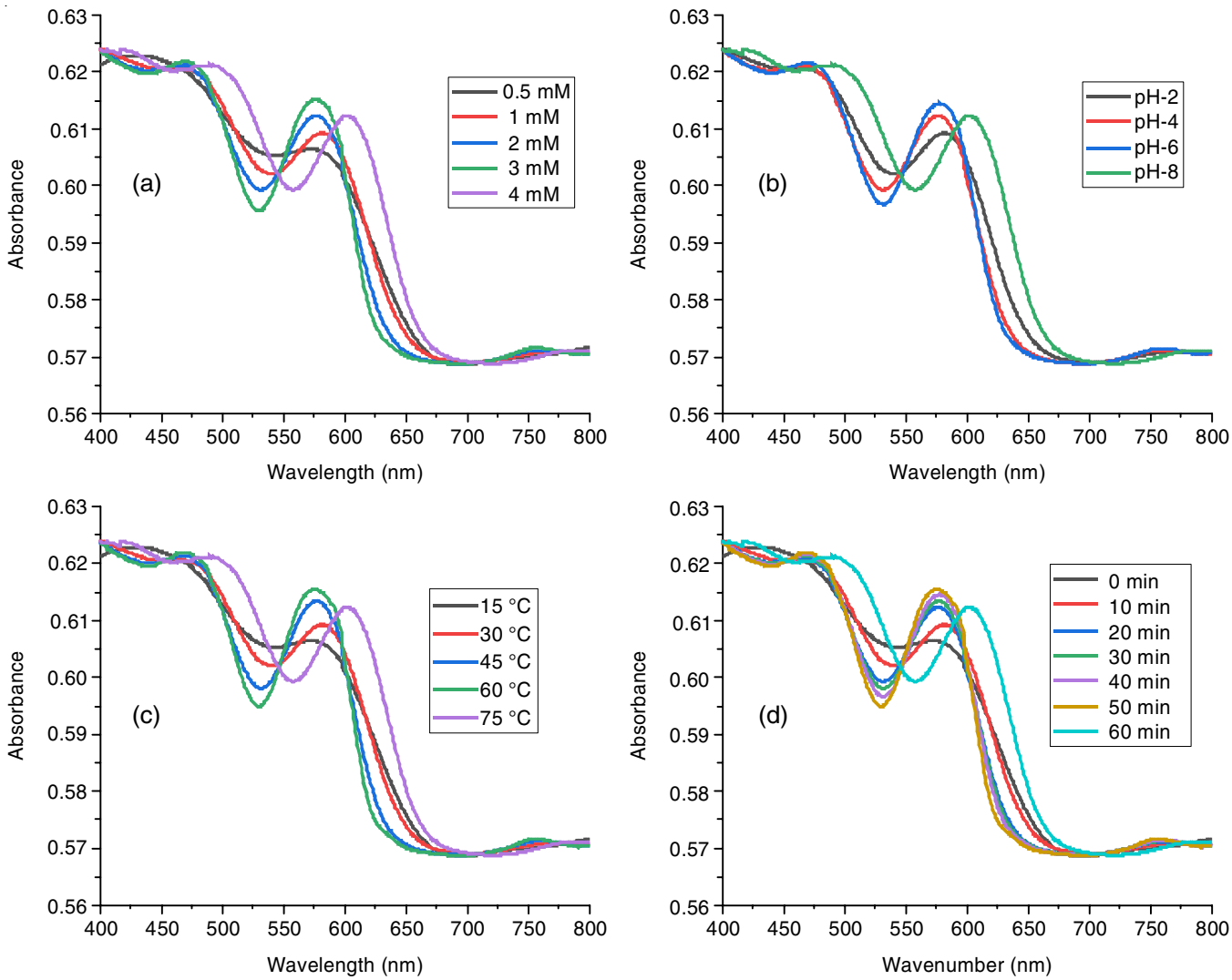

Fig. 2. Influence of precursor concentration, pH, reaction temperature and reaction time

TABLE-1
COMPRESSION OF EXPERIMENTAL &
STANDARD DIFFRACTION ANGLE OF CuNPs

Experimental diffraction angle 2θ (°)	Standard diffraction angle 2θ (°) JCPDS Copper card No: 04-0836
43.0833	43.297
50.4183	50.433
73.9975	74.130

presence of non-homogeneity particles with some agglomeration due to sampling of smaller particles (Fig. 6a). The size of the particles was calculated by the SEM analysis was found to be in the range of 0.43-5.24 µm with an average particle diameter of 5.24 µm [37].

The EDX spectrum confirmed the successful formation of CuNPs with the aqueous fruit extract of *T. chebula* (Fig. 6b). The presence of carbon (C), oxygen (O), nitrogen (N) and copper is depicted in the EDX spectrum (Cu). The presence of an oxygen peak alongside the Cu signal suggested that the CuNPs were capped by phytoconstituents *via* oxygen atoms, whereas the presence of a carbon peak indicated that plant phytochemical groups were involved in the reduction and capping of the synthesized CuNPs [38]. The previous studies carried out for individual spherical-shaped CuNPs also show strong signal peaks at 1.0 and 8.0 keV [39].

Transmission electron microscopy (TEM) studies: The TEM image of *T. chebula* copper nanoparticles (Fig. 7a) revealed that CuNPs were spherical and an average size of 23.68 nm (Fig. 7b) [37]. The selected area electron diffraction (SAED) pattern of CuNPs is shown in Fig. 7c. The selected area electron diffraction (SAED) pattern showed bright circular fringes confirming a good crystalline. The interplanar spacing (d-spacing) was calculated to be 0.209 nm indicating the preferred (111) orientation.

Scavenging activity of biosynthesized copper nanoparticles: Anti-oxidant activity of TC-CuNPs was assessed by DPPH free radical scavenging assays. TC-CuNPs has shown potent DPPH radical scavenging activity and it was exhibited in a dose-dependent manner (Fig. 8a-b). It shows that anti-oxidant activity was directly proportional to the concentration of TC-CuNPs as shown in Table-2. The EC_{50} (effective concentration required to inhibit 50% of free radicals) of TC-CuNPs was determined as 44.65 µg/mL for DPPH radical scavenging

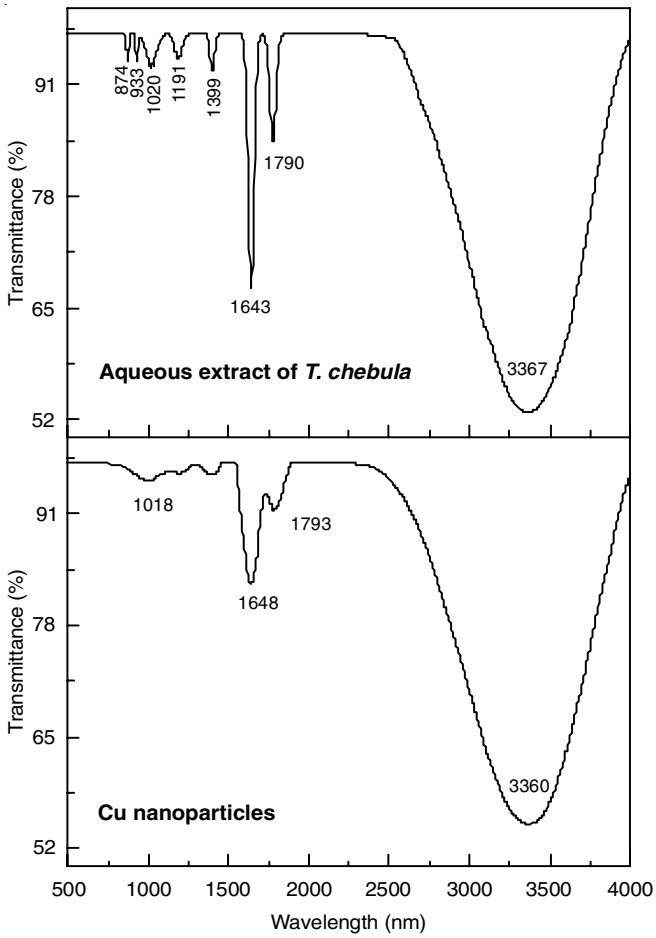

Fig. 3. FTIR of *T. chebula* fruit aqueous extract and CuNPs

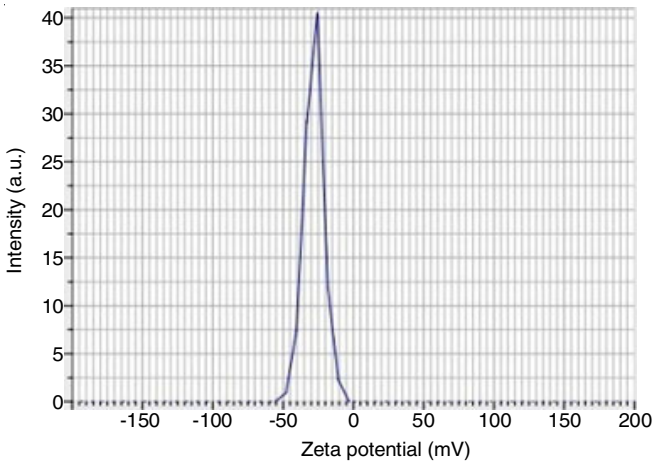

Fig. 4. Zeta-potential record of biosynthesized CuNPs

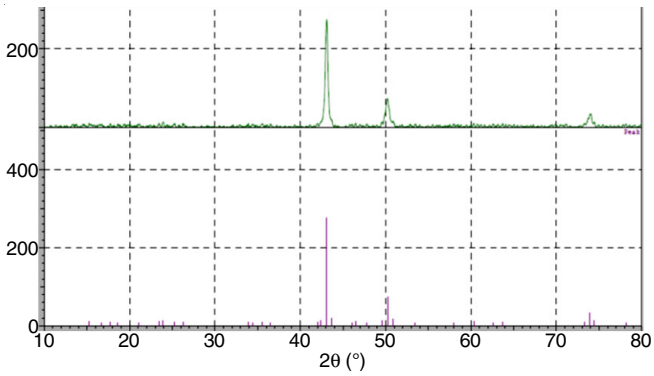

Fig. 5. XRD diffraction pattern of CuNPs indicating the growth of particles in monoclinic crystal structure

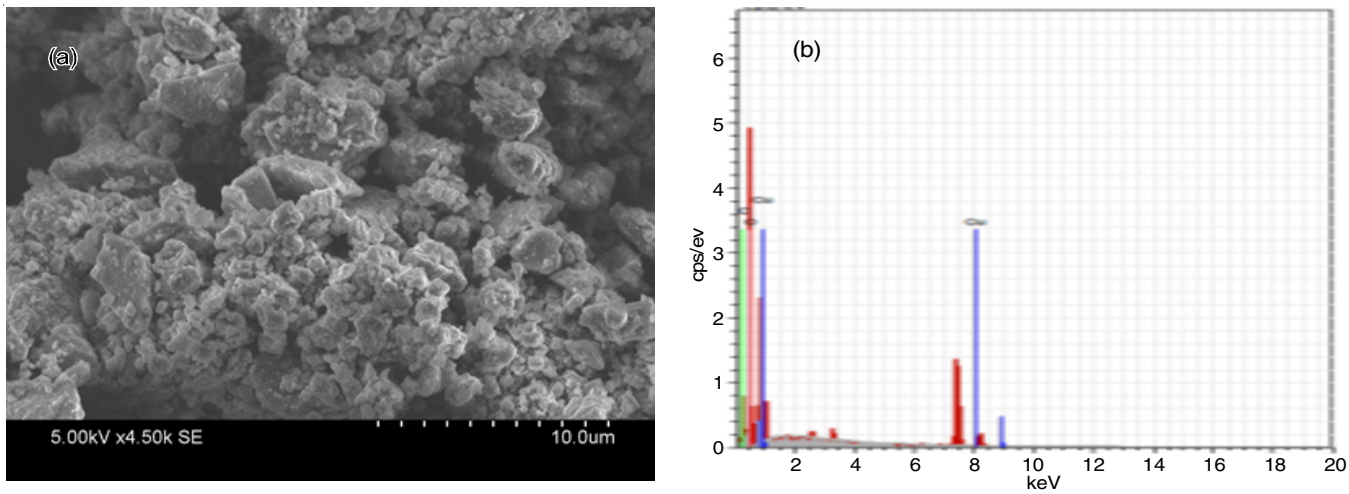

Fig. 6. (a) SEM images of CuNPs, (b) EDAX analysis of CuNPs

TABLE-2
SCAVENGING ACTIVITY OF ASCORBIC ACID AND BIOSYNTHESIZED CuNPs

Volume of DPPH (mL)	Concentration of ascorbic acid (µg/mL)	Concentration of CuNPs (µg/mL)	% AA of ascorbic acid (%)	LC_{50} of ascorbic acid	% of AA of CuNPs	LC_{50} of CuNPs
3	10	10	16.34		9.42	
3	20	20	44.23	26.28	14.11	44.65
3	30	30	55.76		27.65	
3	40	40	76.92		45.5	
3	50	50	90.38		58.5	

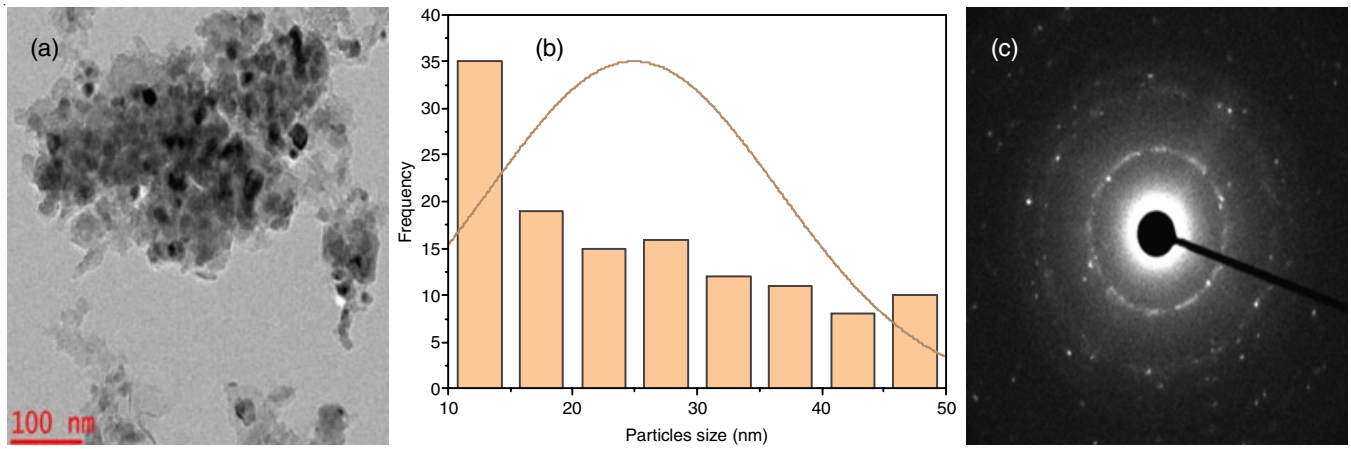

Fig. 7. (a) TEM image of CuNPs, (b) Particle size distribution of CuNPs, (c) SAED Pattern of CuNPs

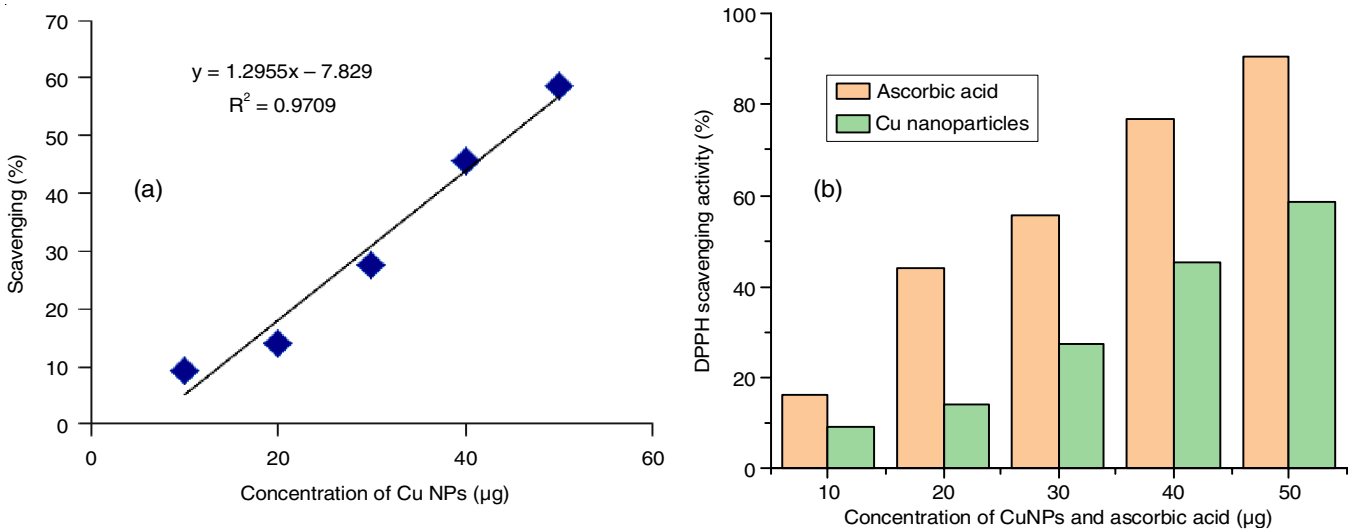

Fig. 8. (a) Plot of scavenging activity of copper nanoparticles (CuNPs), (b) scavenging activity of CuNPs and ascorbic acid

activity and the EC_{50} value of ascorbic acid (reference standard) was 26.28 µg/mL for DPPH radical scavenging activity, respectively. Though, among the different concentrations of CuNPs tested, the highest scavenging activity (58.5 %) was obtained for 50 µg/mL and the lowest scavenging effect (9.42%) was observed for 10 µg/mL. Dose-dependent antioxidant activity of CuNPs was observed. Hence, the TC-CuNPs exhibited effective antioxidant activity as like ascorbic acid [12].

Antibacterial activity: The antibacterial activity of biosynthesized CuNPs against the human pathogens showed varied levels of inhibitions minimum inhibitory concentration (MIC) are shown in Table-3 and the present study revealed that CuNPs showed potential antibacterial activity against *E. coli* (14.5 mm) and *S. aureus* (9.2 mm). The nanoparticles showed maximum zone of inhibition against *E. coli*. The TC-CuNPs showed a higher toxicity for Gram-negative bacteria compared to Gram-positive bacteria [40]. Microdilution method was used to determine the lowest concentration of nanoparticles that was inhibiting the growth of *E. coli* (21.83 ± 1.56 µg/mL) and *S. aureus* (16.16 ± 0.76 µg/mL) and determined to be effective in assessing excellent activities [41].

TABLE-3
ANTIBACTERIAL ACTIVITY OF TC-CuNPs AT DIFFERENT CONCENTRATIONS AGAINST PATHOGENS

Pathogen	Concentration of TC-CuNPs (µL)	Inhibition zone (mm)	MIC (µg/mL)
E. coli	40	2	21.83 ± 1.56
	60	4	
	80	6	
	100	14.5	
S. aureus	40	2	16.16 ± 0.76
	60	4	
	80	8	
	100	9.2	

When compared to previous work reported by many researchers, the antimicrobial results obtained using TC-CuNPs were found to be superior (Table-4). The maximum zone of inhibition (mm) observed with TC-CuNPs against *E. coli* bacteria was found to be 14.5 mm, which is much higher than the zone of inhibition displayed by CuNPs synthesized from other plant extracts (Table-4).

TABLE-4
COMPARATIVE STATISTICS OF ANTIMICROBIAL ACTIVITIES OF CuNPs SYNTHESIZED BY USING VARIOUS PLANT EXTRACTS

Plant extract	Inhibition zone (mm)	Tested Pathogen	Ref
Syzygium aromaticum bud extract	7	*E. coli*	[21]
Ziziphus spina-christi (L.) Willd. fruit extract	13	*E. coli*	[5]
Hagenia abyssinica (Brace) JF. Gmel. leaf extract	12	*E. coli*	[37]
Black grape leaf extract	14	*E. coli*	[28]
Terminalia chebula fruit aqueous extract	14.5	*E. coli*	Present work
Ziziphus spina-christi (L.) Willd. fruit extract	13	*S. aureus*	[5]
Green and black tea leaf extract	14	*S. aureus*	[11]
Hagenia abyssinica (Brace) JF. Gmel. leaf extract	14.7	*S. aureus*	[37]
Terminalia chebula fruit aqueous extract	10	*S. aureus*	Present work

Conclusion

Present study revealed that the aqueous extract of *Terminalic chebula* fruit facilitates the simple, quick, cost-effective and eco-friendly synthesis of copper nanoparticles (CuNPs). The formation of green CuNPs was initially recognized by using a UV-visible spectrophotometer and the role of phytochemicals was confirmed with FTIR, zeta potential and EDX analyses. The XRD analysis confirmed the crystalline nature (FCC) of CuNPs and TEM results has revealed spherical shapes and sizes of around 23.68 nm. The biosynthesized CuNPs shown significant antioxidant activity against DPPH and the anti-bacterial efficacy against *E. coli* (Gram-negative bacteria) and *S. aureus* (Gram-positive bacteria) indicated that the zone of inhibition was greater in Gram-negative bacteria than in Gram-positive bacteria. Finally, the synergistic action of bioactive chemicals from medicinal plants combined with CuNPs has been shown to be effective against infections.

CONFLICT OF INTEREST

The authors declare that there is no conflict of interests regarding the publication of this article.

REFERENCES

1. P. Singh, Y.-J. Kim, D. Zhang and D.-C. Yang, *Trends Biotechnol.*, **34**, 588 (2016); https://doi.org/10.1016/j.tibtech.2016.02.006
2. G. Sharma, A. Kumar, S. Sharma, M. Naushad, R.P. Dwivedi, Z.A. Al-Othman and G.T. Mola, *J. King Saud Univ. Sci.*, **31**, 257 (2019); https://doi.org/10.1016/j.jksus.2017.06.012
3. S. Bayda, M. Adeel, T. Tuccinardi, M. Cordani and F. Rizzolio, *Molecules*, **25**, 112 (2020); https://doi.org/10.3390/molecules25010112
4. M.A. Gatoo, S. Naseem, M.Y. Arfat, A.M. Dar, K. Qasim and S. Zubair, *Toxicity of Nanomater.*, **2014**, 498420 (2014); https://doi.org/10.1155/2014/498420
5. N. Kulkarni and U. Muddapur, *J. Nanotechnol.*, **2014**, 510246 (2014); https://doi.org/10.1155/2014/510246
6. K. Gopinath, S. Kumaraguru, K. Bhakyaraj, S. Mohan, K.S. Venkatesh, M. Esakkirajan, P. Kaleeswarran, N.S. Alharbi, S. Kadaikunnan, M. Govindarajan, G. Benelli and A. Arumugam, *Microb. Pathog.*, **101**, 1 (2016); https://doi.org/10.1016/j.micpath.2016.10.011
7. B.V. Kumar, P. Taj and K.H. Reddy, *Asian J. Chem.*, **32**, (2020); https://doi.org/10.14233/ajchem.2020.22761.
8. S. Wu, S. Rajeshkumar, M. Madasamy and V. Mahendran, *Artif. Cells Nanomed. Biotechnol.*, **48**, 1153 (2020); https://doi.org/10.1080/21691401.2020.1817053
9. S.C. Kotval, T. John and K.A. Parmar, *J. Nanosci. Technol.*, **4**, 456 (2018); https://doi.org/10.30799/jnst.133.18040415
10. N.I. Hulkoti and T.C. Taranath, *Colloids Surf. B Biointerfaces*, **121**, 474 (2014); https://doi.org/10.1016/j.colsurfb.2014.05.027
11. M. Ponnanikajamideen, S. Rajeshkumar, M. Vanaja and G. Annadurai, *Can. J. Diabetes*, **43**, 82 (2019); https://doi.org/10.1016/j.jcjd.2018.05.006
12. M.I. Din, F. Arshad, Z. Hussain and M. Mukhtar, *Nanoscale Res. Lett.*, **12**, 638 (2017); https://doi.org/10.1186/s11671-017-2399-8
13. G. Balakrishnan, S. Shil, N. Vijalakashmi, M.R.K. Rao and K. Prabhu, *Drug Invent. Today*, **12**, 2038 (2019).
14. A.H. Abbas and N.Y. Fairouz, *Mater. Today Proc.*, **61**, 908 (2022); https://doi.org/10.1016/j.matpr.2021.09.551
15. N. Sebeia, M. Jabli and A. Ghith, *Inorg. Chem. Commun.*, **105**, 36 (2019); https://doi.org/10.1016/j.inoche.2019.04.023
16. B. Khodashenas and H.R. Ghorbani, *Arab. J. Chem.*, **12**, 1823 (2019); https://doi.org/10.1016/j.arabjc.2014.12.014
17. V. Kulkarni, S. Suryawanshi and P. Kulkarni, *Curr. Sci.*, **109**, 257 (2015).
18. M. Nilavukkarasi, S. Vijayakumar and S.P. Kumar, *Mater. Sci. Energy Technol.*, **3**, 371 (2020); https://doi.org/10.1016/j.mset.2020.02.008
19. S. Shende, A.P. Ingle, A. Gade and M. Rai, *World J. Microbiol. Biotechnol.*, **31**, 865 (2015); https://doi.org/10.1007/s11274-015-1840-3
20. M. Nasrollahzadeh, S.M. Sajadi and M. Khalaj, *RSC Adv.*, **4**, 47313 (2014); https://doi.org/10.1039/C4RA08863H
21. K.M. Rajesh, B. Ajitha, Y.A. Kumar Reddy, Y. Suneetha and S. Reddy, *Optik*, **154**, 593 (2018); https://doi.org/10.1016/j.ijleo.2017.10.074
22. P.C. Gupta, *Int. J. Pharm. Pharm. Sci.*, **4(Suppl.3)**, 62 (2012).
23. K. Mohan Kumar, B.K. Mandal, M. Sinha and V. Krishnakumar, *Spectrochim. Acta A Mol. Biomol. Spectrosc.*, **86**, 490 (2012); https://doi.org/10.1016/j.saa.2011.11.001
24. A. Altemimi, N. Lakhssassi, A. Baharlouei, D.G. Watson and D.A. Lightfoot, *Plants*, **6**, 42 (2017); https://doi.org/10.3390/plants6040042
25. M. Khan, K. Al-hamoud, Z. Liaqat, M.R. Shaik, S.F. Adil, M. Kuniyil, H.Z. Alkhathlan, A. Al-Warthan, M.R.H. Siddiqui, M. Mondeshki, W. Tremel, M. Khan and M.N. Tahir, *Nanomaterials*, **10**, 1885 (2020); https://doi.org/10.3390/nano10091885
26. D. Muralidharan, A.J. Raiza and K. Pandian, *Asian J. Chem.*, **33**, 2049 (2021). https://doi.org/10.14233/ajchem.2021.23295
27. P. Deepthi, P.N. Kumar and P. Prema, *Indian J. Chem. Technol.*, **28**, 123 (2021).
28. T. Alam, S. Tyagi, G. Kumar, A. Khan, N. Chauhan, H. Tarannum, P. Ahmad and A. Rizvi, *Asian J. Chem.*, **32**, 2229 (2020); https://doi.org/10.14233/ajchem.2020.22738
29. N.A. Thamer, N.Q. Muftin and S.H.N. Al-Rubae, *Asian J. Chem.*, **30**, 1559 (2018); https://doi.org/10.14233/ajchem.2018.21242
30. X. Huang and M.A. El-Sayed, *J. Adv. Res.*, **1**, 13 (2010); https://doi.org/10.1016/j.jare.2010.02.002
31. M.R. Salvadori, L.F. Lepre, R.A. Ando, C.A. Oller do Nascimento and B. Corrêa, *PLoS One*, **8**, e80519 (2013); https://doi.org/10.1371/journal.pone.0080519

32. S. Amaliyah, D.P. Pangesti, M. Masruri, A. Sabarudin and S.B. Sumitro, *Heliyon*, **6**, e04636 (2020); https://doi.org/10.1016/j.heliyon.2020.e04636
33. M.I. Din, A.G. Nabi, A. Rani, A. Aihetasham and M. Mukhtar, *Environ. Nanotechnol. Monit. Manag.*, **9**, 29 (2018); https://doi.org/10.1016/j.enmm.2017.11.005
34. Nayantara and P. Kaur, *Biotechnol. Res. Innov.*, **2**, 63 (2018). https://doi.org/10.1016/j.biori.2018.09.003
35. S.C. Mali, A. Dhaka, C.K. Githala and R. Trivedi, *Biotechnol. Rep.*, **27**, e00518 (2020); https://doi.org/10.1016/j.btre.2020.e00518
36. T. Theivasanthi and M. Alagar, *Scholars Res. Lib.*, **1**, 112 (2010).
37. H.C.A. Murthy, T. Desalegn, M. Kassa, B. Abebe and T. Assefa, *J. Nanomater.*, **2020**, 3924081 (2020); https://doi.org/10.1155/2020/3924081
38. M. Khodaie and N. Ghasemi, *Bulg. Chem. Commun.*, **50**, 244 (2018).
39. M. Ismail, S. Gul, M.I. Khan, M.A. Khan, A.M. Asiri and S.B. Khan, *Green Process. Synth.*, **8**, 135 (2019); https://doi.org/10.1515/gps-2018-0038
40. W. Ren, Z. Qiao, H. Wang, L. Zhu and L. Zhang, *Med. Res. Rev.*, **23**, 519 (2003); https://doi.org/10.1002/med.10033
41. K. Mandava, K. Kadimcharla, N.R. Keesara, S.N. Fatima, P. Bommena and U.R. Batchu, *Indian J. Pharm. Sci.*, **79**, 695 (2017); https://doi.org/10.4172/pharmaceutical-sciences.1000281